Parasites & Vectors

RESEARCH

Open Access

Identification of differentially expressed genes based on antennae RNA-seq analyses in *Culex quinquefasciatus* and *Culex pipiens molestus*

Heting Gao†, Zhenyu Gu†, Dan Xing†, Qiaojiang Yang, Jianhang Li, Xinyu Zhou, Teng Zhao* and Chunxiao Li*

Abstract

Background: Both *Culex quinquefasciatus* and *Cx. pipiens molestus* are sibling species within *Cx. pipiens* complex. Even though they are hard to distinguish morphologically, they have different physiological behaviors. However, the molecular mechanisms underlying these differences remain poorly understood.

Methods: Transcriptome sequencing was conducted on antennae of two sibling species. The identification of the differentially expressed genes (DEGs) was performed by the software DESeq2. Database for Annotation, Visualization and Integrated Discovery was used to perform GO pathway enrichment analysis. The protein–protein interaction (PPI) network was constructed with Cytoscape software. The hub genes were screened by the CytoHubba plugin and Degree algorithms. The identified genes were verified by quantitative real-time PCR.

Results: Most annotated transcripts (14,687/16,005) were expressed in both sibling species. Among 15 identified odorant-related DEGs, *OBP10* was expressed 17.17 fold higher in *Cx. pipiens molestus* than *Cx. quinquefasciatus*. Eighteen resistance-related DEGs were identified, including 15 from *CYP* gene family and three from acetylcholinesterase, in which *CYP4d1* was 86.59 fold more highly expressed in *C. quinquefasciatus*. Three reproductive DEGs were indentified with the expression from 5.01 to 6.55 fold. Among eight vision-related DEGs, retinoic acid receptor RXR-gamma in *Cx. pipiens molestus* group was more expressed with 214.08 fold. Among the 30 hub genes, there are 10 olfactory-related DEGs, 16 resistance-related DEGs, and four vision-related DEGs, with the highest score hub genes being *OBP lush* (6041148), *CYP4C21* (6044704), and *Rdh12* (6043932). The RT-qPCR results were consistent with the transcriptomic data with the correlation coefficient $R = 0.78$.

Conclusion: The study provided clues that antennae might play special roles in reproduction, drug resistance, and vision, not only the traditional olfactory function. *OBP lush*, *CYP4C21*, and *Rdh12* may be key hints to the potential molecular mechanisms behind the two sibling species' biological differences.

Keywords: Mosquitoes, Antennae, Olfactory, Reproduction, Resistance, Vision, RNA-seq

Background

Mosquitoes are not only annoying but can also transmit pathogens, resulting in billions of potential infections and approximately 700,000 deaths worldwide each year. Different species of mosquitoes carry and transmit different pathogens [1, 2]. For example, some species of

†Heting Gao, Zhenyu Gu and Dan Xing have contributed equally to this work

*Correspondence: zhaoteng2013@163.com; aedes@126.com

State Key Laboratory of Pathogen and Biosecurity, Beijing Key Laboratory of Vector Borne and Natural Focus Infectious Disease, Beijing 100071, China

Culex mosquitos are vectors of West Nile virus, Japanese encephalitis virus, and lymphatic filariasis [3].

Culex quinquefasciatus (*Cx. quinquefasciatus*, Cqui) and *Cx. pipiens molestus* (*Cx. p. molestus*, Cmls) are sibling species within *Cx. pipiens complex* whose morphologies are difficult to distinguish [4]. However, *Cx. p. molestus* and *Cx. quinquefasciatus* have very different physiological behaviors. For example, *Cx. p. molestus* mainly mate in confined spaces. Their ovaries can develop normally, and they lay eggs without blood-feeding in their first life cycle. On the other hand, *Cx. quinquefasciatus* mate in open areas. There are also differences in their preference for mammalian and bird blood sources [5]. Although the different blood-feeding habits and other physiological behaviors of the two sibling species have been observed for a long time, their possible molecular mechanisms have still not been totally illustrated.

Antenna is the main chemosensory organ of mosquito and plays an important role in smell [6], hearing [7], host-locating [8], and courtship [9]. The mosquito antenna comprises three parts: scape, pedicel, and flagellum. The antenna and maxillary palp detect odors emanating from the host. With the help of proboscis and eyes, which detect taste and visual cues, mosquitoes are successful in flight navigation toward the host [10]. The expressions of many chemoreceptor genes have been found in the antennae of *Anopheles sinensis*, and their expression levels are significantly regulated after the blood meal [11], quite similar to the antennae of the *Culex pipiens* complex [12] and *Aedes aegypti* [13–15]. Besides the typical olfactory function, the antennae of mosquitoes are model systems for other sensations, including acoustics [16].

We conducted transcriptome sequencing on antennae of *Cx. p. molestus* and *Cx. quinquefasciatus* and then explored the differences in the expression and interaction of transcripts. Besides olfaction, antennae could also have special roles in reproduction, drug resistance, and visual function. The study provides hints about the potential molecular mechanisms behind the two sibling species' biological differences.

Methods

Mosquitoes

Both *Cx. p. molestus* and *Cx. quinquefasciatus* were obtained from long-term laboratory-reared strains, which had been characterized by male genitalia and/or cytochrome oxidase subunit I (*COI*) barcoding in advance [17, 18]. The breeding conditions were as follows: temperature 26 ± 1 °C, relative humidity 70 ± 5%, and a light:dark regime 14 h:10 h.

RNA extraction and library construction

Two groups of samples were designed in this study: antennae of *Cx. quinquefasciatus* (Cqui) and antennae of *Cx. p. molestus* (Cmls). Biological samples containing 50 antennae were set in four replicates for each group. RNA was extracted with TRIzol (Takara.9108). Libraries were constructed using the NEB Next Ultra RNA Library Prep Kit and finally sent to Beijing Macro-Micro-test Biotechnology Co., Ltd., for transcriptome sequencing.

Transcriptome sequencing analysis

After the raw data were filtered, clean reads were compared to the reference genome using HISAT2 software [19]. Reference genome file was acquired from the data in the National Center for Biotechnology Information (NCBI)(GCF_015732765.1) [20, 21]. Transcript assembly was performed with StringTie software [22] followed by annotation from databases such as P fam [23], Gene Ontology (GO) [24, 25], and the Kyoto Encyclopedia of Genes and Genomes (KEGG) [26].

A differential analysis was performed using DESeq2 software [27]. The screening criteria for differentially expressed genes (DEGs) in antennae were $padj < 0.05$ *and* $|log2(foldchange)| > 1$. Functional annotation and GO enrichment analyses were carried out using the R and clusterProfiler [28, 29] to categorize the DEGs into biological process (BP), molecular function (MF), and cellular components (CC).

Protein-protein interaction (PPI) network analysis obtained the interaction network file through the STRING database [30]. The files were displayed using Cytoscape software [31]. The cytoHubba plug-in Degree topology algorithm was used to predict and explore to calculate gene scores for hub genes [32].

qPCR verification of identified DEGs

Ten genes with relatively high expressions and significant differences were randomly selected and combined with housekeeping genes 18S ribosomal RNA (*18S*) to verify the accuracy of the transcriptome results. The primers were designed with Oligo Primer Analysis software version 4.0 (Additional file 1: Table S1). A qPCR analysis was conducted with a One Step SYBR PrimeScript RT-PCR Kit II (Cat# RR086A, Takara). The reaction conditions were set as follows: 94 °C for 30 s, 94 °C for 5 s, and 60 °C for 30 s, repeated for 40 cycles. Three technical replicates were performed for each sample. The $2^{-\Delta\Delta CT}$ method was applied to calculate the relative gene expression [33, 34]. A chi-square test was used to confirm the pairwise differences at the significance level of $\alpha = 0.05$. The correlation

between RNA-seq and RT-qPCR expression was calculated by Pearson correlation.

Result

Sequencing data quality

After sample data were filtered and the adapter removed, the metagenomic sequencing depth of eight samples was around 30G. The number of valid reads ranged from 22876221 to 31754347. There were 206232097 reads (16,005 annotated transcripts) in total. The Q20 values were all > 95%, suggesting a high degree of quality (Table 1).

Transcriptome differential expression analysis of antennae

Principal component analysis showed that the ellipse represented the grouping area with 68% confidence interval; all biological replicates of Cqui and Cmls sample were distributed in two distinct groups (Fig. 1A). Most annotated transcripts (14,687/16,005) were expressed in both sibling species. The number of *Cx. quinquefasciatus*- and *Cx. p. molestus*-specific transcripts were 890 and 428, respectively (Fig. 1B). There were 1577 DEGs in the antennal transcriptome of Cqui and Cmls, of which 1166 DEGs were more highly expressed in the Cqui group and 411 DEGs were higher in the Cmls group (Fig. 1C).

With the purpose of better understanding the differences in regulation between the two sibling mosquito species' antennae, we mapped all transcripts to GO pathways to exploit the pathways that were significantly enriched. DEGs with higher expression in the Cqui were enriched in signal transduction, cell communication in BP; channel complex and neural synapse in CC; signaling receptor activity and channel activity in MF (Fig. 1D). DEGs with higher expression in the Cmls group were enriched in defense response, carbohydrate metabolic process in BP; cell projection, component of endoplasmic reticulum membrane in CC; oxidoreductase activity and ion binding pathways in MF (Fig. 1E).

Table 1 Transcriptome sequencing data mapping summary

Sample	Reads number	Alignment rate (%)	Q20 (%)	GC (%)
Cmls_1	25985588	58.55	97.22	53.16
Cmls_2	24538832	57.97	96.82	52.32
Cmls_3	30471828	60.04	96.1	53.74
Cmls_4	31754347	59.27	95.55	53.86
Cqui_1	23234291	57.02	96.58	53.9
Cqui_2	23513630	57.20	95.1	52.61
Cqui_3	23857360	59.69	95.41	53.01
Cqui_4	22876221	59.47	96.63	54.44

Cmls = antennae of *Cx. p. molestus*; Cqui = antennae of *Cx. quinquefasciatu*. Alignment rate indicated the ratio of sequencing results to reference genome. Q20 = proportion of base mass values ≥ 20. GC = proportion of GC bases in the sequencing result

Specific functional DEGs in antennal transcriptome

By further mining the data, we focused on four types of specific functional DEGs, which would affect the key physiological behaviors of mosquitoes, including olfactory, resistance, reproduction, and vision. A total of 15 odorant-related DEGs were identified, of which 11 were more highly expressed in the Cqui group and four more highly expressed in the Cmls group. Most (12/15) were odorant-binding proteins (*OBP*); two other DEGs (*OR67d* and *OR7a*) were odorant receptors (*OR*) and one (*GR22*) a gustatory receptor (*GR*). Of these, *OBP10* in cmls groups were specially more highly expressed at 17.17 fold times compared with the Cqui group (Fig. 2A, Additional file 1: Table S2).

A total of 18 resistance-related DEGs were identified, including 15 from cytochrome P450 (*CYP*) gene family and three from acetylcholinesterase (*AchE*). Eight *CYP* family DEGs were more expressed in Cqui; for example, *CYP4D1* was 86.59 fold more highly expressed. Three *AchE* genes were differentially expressed with fold change ranging from 0.39–4.59 (Fig. 2B, Additional file 1: Table S3).

Two related vitellogenin-A1 (*Vg-A1*) and one location of vulva defective 1 (*lov-1*) DEGs were more expressed in the Cmls, with expression from 5.01 to 6.55 fold. These three genes were all related to insect mating (Fig. 2C, Additional file 1: Table S4).

Four vision-related genes were more expressed in the Cqui group and four more expressed in the Cmls group. Typically, retinoic acid receptor (*RAR*) RXR-gamma in Cmls group was more expressed at 214.08 fold. Vertebrate ancient (VA) opsin in Cqui group was more expressed with 12.43 fold change (Fig. 2D, Additional file 1: Table S5).

(See figure on next page.)

Fig. 1 **A** Principal component analysis of the antennal RNA-Seq data of Cqui and Cmls. **B** Venn diagram for two sibling species transcrips. **C** Volcano plot analysis of DEGs between antennal transcriptomes. Green dots indicate DEGs with higher expression in Cqui group, and red dots indicate DEGs with higher expression in Cmls group. **D** GO enrichment analysis of DEGs more expressed in Cqui group. **E** GO enrichment analysis of DEGs more expressed in Cmls group

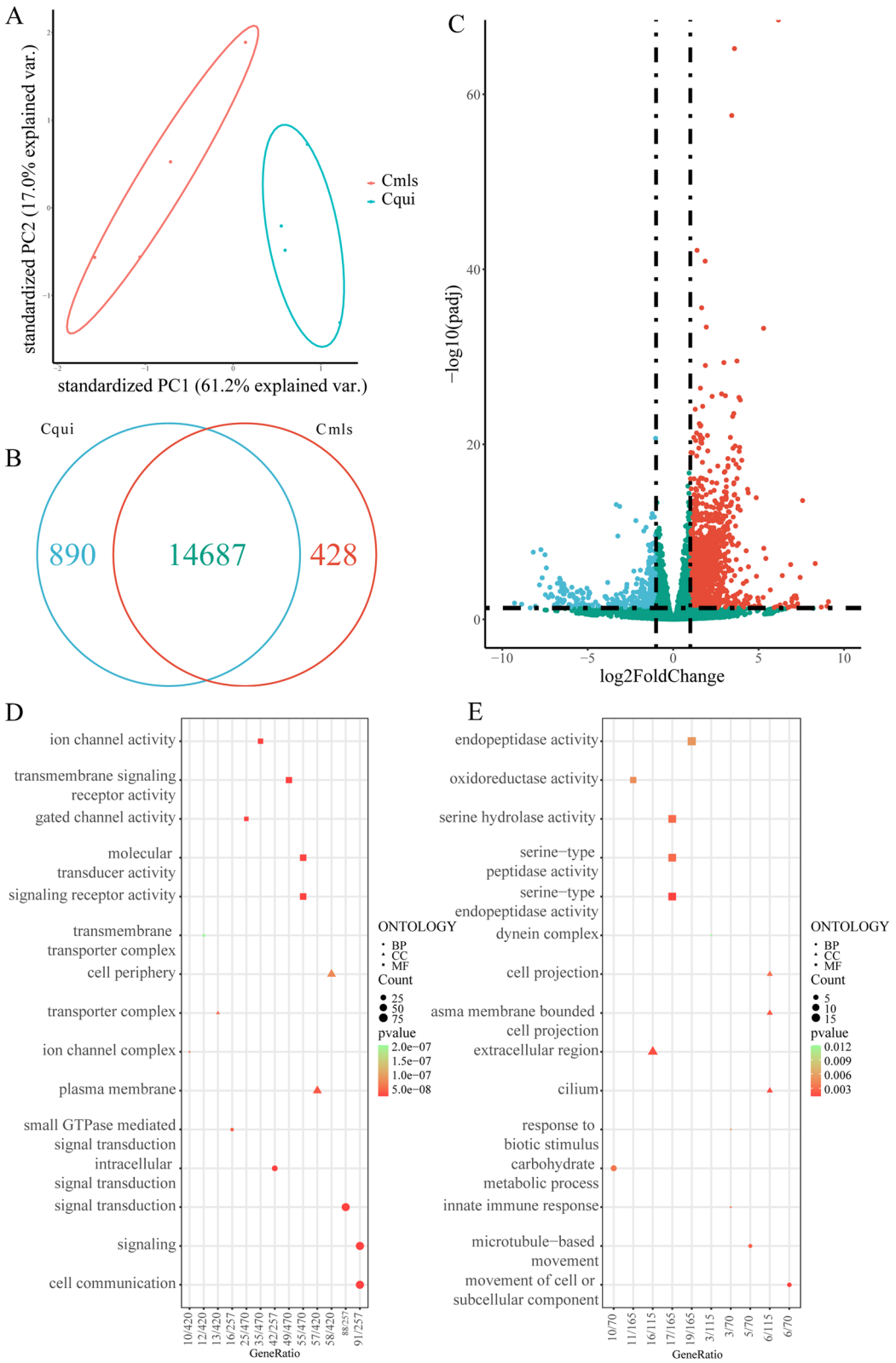

Fig. 1 (See legend on previous page.)

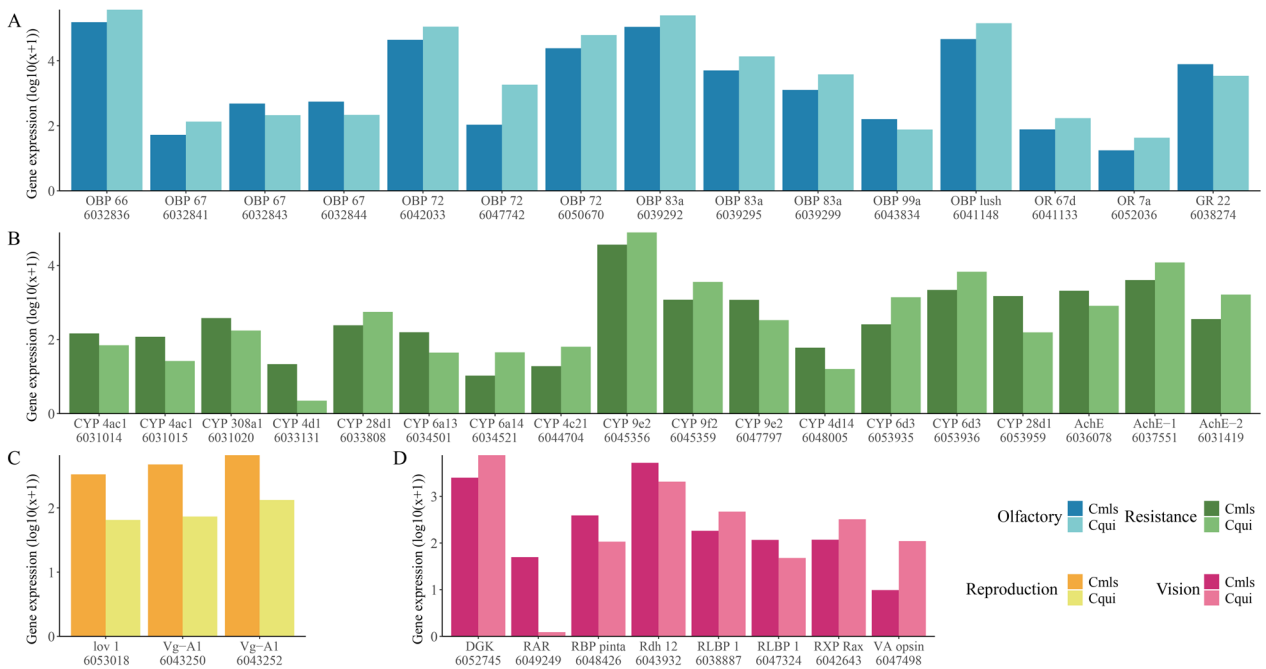

Fig.2 Expression level for specific functional DEGs. Light color-filled columns represent the gene expression of Cqui group; dark color-filled columns represent the gene expression of Cmls group. **A** Expression level of olfactory-related DEGs. **B** Expression level of resistance-related DEGs. **C** Expression level of reproduction-related DEGs. **D** Expression level of visual-related DEGs

PPI network for specific functional hub genes

Hub genes were the nodes with higher degree, i.e. nodes with more connections in related pathways. With the cytoHubba plug-in and the Degree algorithm, we calculated the hub gene and drew the PPI Networks, PPI (Fig. 3A). PPI was mainly divided into four parts: *CYP* family, olfactory-related genes (*OR*, *OBP*, and *GR*) and *AchE* family and vision-related genes (*RBP* and *Rdh*). The highest scores for specific functional hub genes were *CYP4C21* (6044704), *OBP lush* (6041148), and *Rdh12* (6043932), respectively. Hub genes were closely related internally in each specific function. The hub gene score and function are presented in Additional file 1: Table S6. Among the 30 hub genes, there were ten olfactory-related DEGs, 16 resistance-related DEGs, and four vision-related DEGs (Fig. 3B).

RT-qPCR validation

To validate the reliability of the DEG results, the expression levels of ten selected transcripts were determined by RT-qPCR with the 18S as an internal reference gene. These genes included *OBP*, *Vg*, *CYP*, and so on. All of these genes were significantly different between Cqui and Cmls group on expression of RNA-seq and RT-qPCR (Fig. 4A). The RT-qPCR results were consistent with the transcriptomic data. The correlation coefficient was $R = 0.78$, the significance coefficient $P = 0.0083 < 0.05$ (Fig. 4B).

Discussion

Most previous studies focused on olfactory genes when conducting transcriptome sequencing on mosquito antennae. For example, 77 *OBPs*, 82 *ORs*, 60 *IRs*, and 30 *GRs* were found in the transcriptome sequencing results of different organs of *A. albopictus* [15]. In the sequencing of the antenna transcriptomes between sibling species *An. coluzzii* and *An. quadriannulatus* [35], *Cx. quinquefasciatus* and *Cx. p. molestus* [12], much olfactory gene expression was significantly regulated to affect host seeking and oviposition.

In this study, 15 odor-related genes were found among the DEGs between *Cx. quinquefasciatus* and *Cx. p. molestus*. Among the olfactory-related DEGs mentioned above, GR22 specifically bound to CO_2 [36], and OBP66, general OBP83a, OBP6, general OBP72, OBP12, OBP5, and OBP10 were present specifically in the antennae [37, 38]. *Culex pipiens molestus* was more interested in mammals and sometimes birds [39, 40]. The blood-sucking host of *Cx. quinquefasciatus* was more widespread, including birds and other vertebrates [41]. These 15 odor-related genes might reflect the different feeding patterns of the two mosquito species.

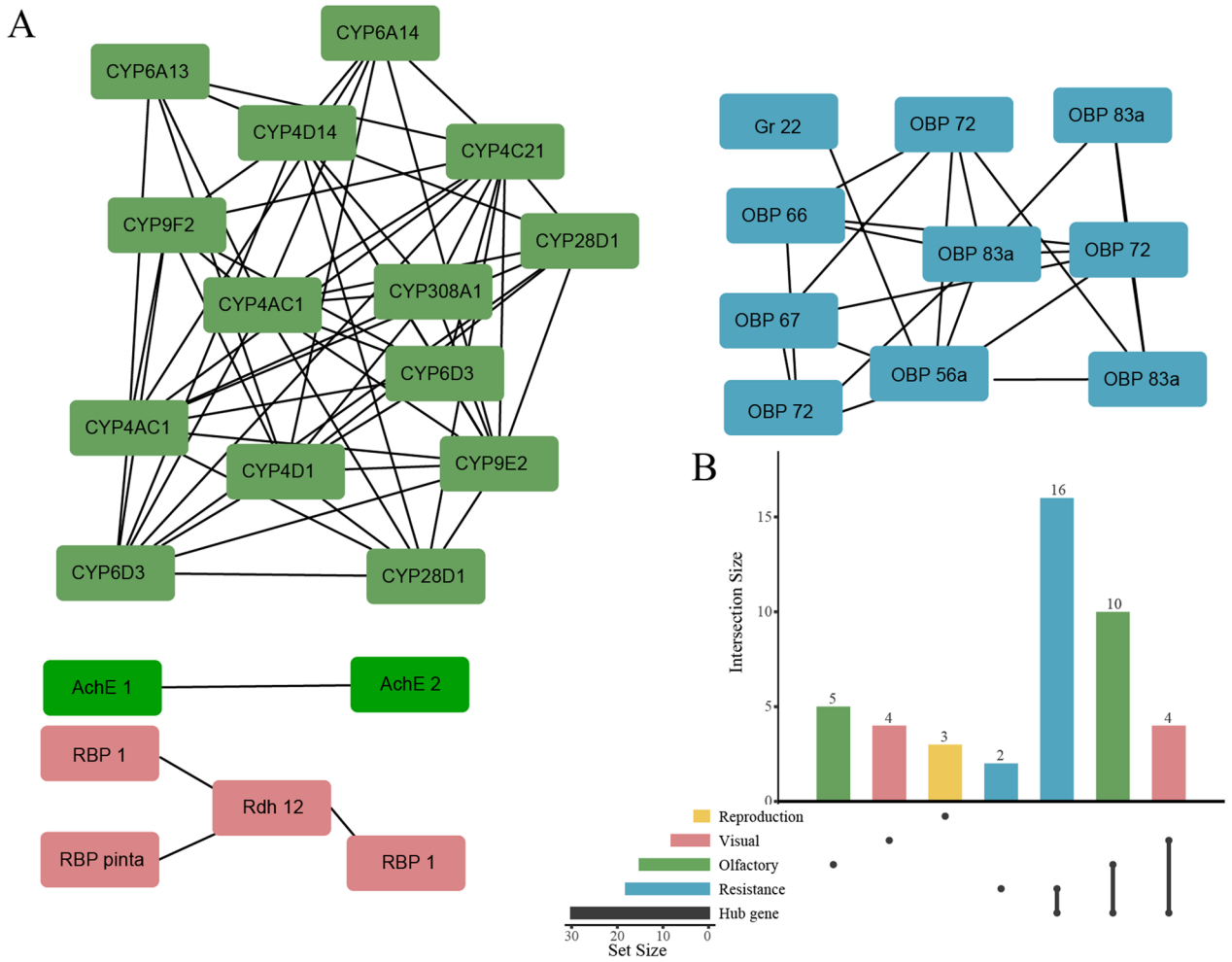

Fig. 3 **A** PPI network of top 30 hub genes related to olfaction, resistance, and vision. Green filling represents the resistance-related gene; red filling represents the vision-related gene; blue filling represents the vision-related gene. **B** The upset plot shows the number of each functional gene in the hub gene

There were 16 resistance-related DEGs in the hub gene PPI network, including genes from *CYP* family and *AchE*. *CYP* superfamily catalyzed various modification reactions, such as oxidation, epoxidation, dehydrogenation, hydrolysis, and reduction [42]. Members of *CYP* played critical roles in the detoxification of xenobiotics such drugs, pesticides, and toxins [43]. *AchE* was an effective insecticide target for mosquito vector control [44]. *CYP4AC1* did not overexpress in *Cx. quinquefasciatus* larvae treated with pyrethroids [45]. *AchE1* had been confirmed to be associated with pyrethroid resistance [46]. Higher expression level of *CYP6AA9* was found responsible for deltamethrin-resistant *Cx. pipiens*. [47]. Our study agreed with previous studies confirming the expression levels of resistance-related genes of *Cx. quinquefasciatus* and *Cx. pipiens pallens* were different [48]. The relationship between 16 resistance-related DEGs and resistance needs further verification.

The two *Vg-A1* genes (6043252,6043250) were highly expressed in *Cx. p. molestus*, which may be related to the autogenous habit [49]. In the absence of a blood meal, the ovaries of *Cx. p. molestus* developed normally, which might have led to higher expression of the *Vg* gene.

Of the eight differentially expressed vision-related genes, *RBP1*, *RXP Rax*, eye-specific *DGK*, and VA opsin were more highly expressed in the Cqui group. Retinal oxide-binding protein was abundantly expressed in locust antenna and associated with olfactory-related behaviors in solitary locusts [50]. Eye-specific *DGK* was essential for the photoreceptor function of the *Drosophila* retina [51, 52]. Vertebrate ancient opsin was a green-sensitive photoreceptor that showed high sequence similarity to vertebrate ancient opsin, which might also have affected

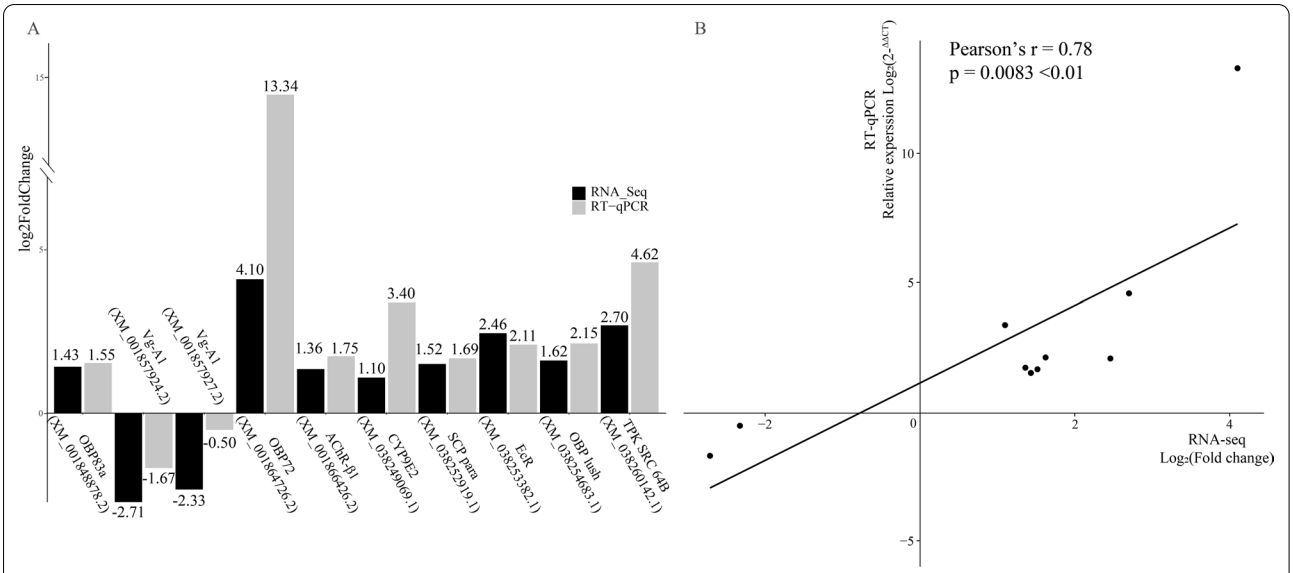

Fig. 4 **A** Verification of DEGs in Cqui group and Cmls group using RT-qPCR. Black-filled columns represent the fold change of gene expression based on comparative transcriptome analysis. Gray-filled columns represent data from RT-qPCR analysis. **B** Correlation between RNA-Seq and RT-qPCR results for the tested DEGs using Pearson correlation coefficient ($P < 0.05$)

sexual maturation [53]. *Rdh12* functioned as part of the visual cycle, which was a series of enzymatic reactions required for the regeneration of the visual pigment and detoxification of lipid peroxidation products [54, 55]. Retinol-binding protein transported vitamin A in the hydrophilic environment of the cytoplasm and regenerated visual pigments [56, 57]. *RAR* was involved in the retinoic acid signaling pathway, which was crucial for the control of embryonic development [58]. The different living environments (*Cx. p. molestus* mated mainly in enclosed spaces, while *Cx. quinquefasciatus* mated mainly in open areas) might interact with the differential expression of their vision-related genes.

GO enrichment results showed that genes with higher expression in *Cx. quinquefasciatus* were mainly enriched in cell communication, G protein-coupled receptor signaling pathway, ion channel complex, cell junction, signaling receptor activity, and other pathways. Previous studies have found that G protein-coupled receptor signaling pathway was closely related to insect feeding behavior [59], which affected insecticide resistance in *Cx. quinquefasciatus* by regulating P450-mediated detoxification [60].

Genes with higher expression in *Cx. p. molestus* were mainly enriched in microtubule-based movement, innate immune response, integral and intrinsic component of endoplasmic reticulum membrane synthesis, and cell division-related pathways. Due to the autogenous habit of *Cx. p. molestus*, the body of *Cx. p. molestus* was richer in carbohydrates, lipids, proteins, and other nutrients [49, 61, 62], with vigorous cell proliferation and stronger immune response.

The screened high scored hub genes would be the key to explore mechanisms behind the two sibling species biological differences. *OBP lush* (6041148) had the highest score for olfactory-related hub gene and consisted of a large family of low-molecular-weight, highly divergent proteins expressed exclusively in the chemosensory sensilla of insects. It was required for normal olfactory behavior in *Drosophila* [63]. *OBP lush* mutant flies were abnormally attracted to high concentrations of ethanol, propanol, and butanol but had normal chemosensory responses to other odorants [64].

The resistance-related hub gene *CYP4C21* (6044704) had the highest score, which was 5.4 times higher in the resistant strain compared with the wild *Ae. aegypti* strain in Vietnam [65]. The hub visual correlation gene with the highest score was *Rdh12* (6043932), an NADPH-dependent retinal reductase, which is expressed in the inner segments of the photoreceptors [54]. *Rdh12* could enzymatically reduce toxic lipid 4-hydroxynonenal in vitro [66], protecting cellular macromolecules against oxidative modification and protecting photoreceptors from light-induced apoptosis [67].

Our transcriptome sequencing on antennae of *Cx. quinquefasciatus* and *Cx. p. molestus*, not only focused on olfactory-related genes in common view, but also expanded the orientation of resistance-, reproduction-, and vision-related genes of two sibling species of mosquitoes. Even though the RT-qPCR results confirmed the

RNA-Seq prediction to some extent, further molecular and behavioral investigations are needed. This study provides hints about the potential molecular mechanisms behind the two sibling species' biological differences, like blood-feeding, detoxication, mating, host-locating, and other physiological behaviors, which could facilitate the design and development of more targeted repellents or insecticides. By interfering with or silencing the specific genes with RNAi or CRISPR techniques, mosquito host localization ability and resistance to insecticides were affected, leading to the decrease of vector competence. The screened key genes can help to control mosquito-borne diseases effectively and efficiently.

Abbreviations

DEGs: Differentially expressed genes; PPI: Protein–protein interaction; qRT-PCR: Quantitative real-time PCR; Cqui: Antennae of *Culex quinquefasciatus*; Cmls: *Culex pipiens molestus*; NCBI: National Center for Biotechnology Information; GO: Gene Ontology; KEGG: Kyoto Encyclopedia of Genes and Genomes; BP: Biological process; MF: Molecular function; CC: Cellular components; 18S: 18S ribosomal RNA; OBP: Odorant-binding protein; OR: Odorant receptor; GR: Gustatory receptor; CYP: Cytochrome P450; AchE: Acetylcholinesterase; Vg: Vitellogenin; lov: Location of vulva defective; RAR: Retinoic acid receptor; VA: Vertebrate ancient; DGK: Eye-specific diacylglycerol kinase; RBP: Retinol-binding protein; Rdh: Retinol dehydrogenase; RLBP: Retinaldehyde-binding protein; RXP: Retinal homeobox protein; AchR: Acetylcholine receptor; SCP: Sodium channel protein; EcR: Ecdysone receptor; TPK: Tyrosine-protein kinase.

Supplementary Information

The online version contains supplementary material available at https://doi.org/10.1186/s13071-022-05482-6.

Additional file 1: Table S1. The qPCR primers designed to verify RNA-seq results. **Table S2.** Olfactory-related differentially expressed genes. **Table S3.** Resistance-related differentially expressed genes. **Table S4.** Reproduction-related differentially expressed genes. **Table S5.** Visual-related differentially expressed genes. **Table S6.** The hub gene score and function.

Author contributions

TZ and CL conceived, designed the experiments, obtained the funding, and revised the manuscript. QY, XZ, and ZG carried out the experiments (RT-qPCR, total RNA extraction, construction of cDNA library). HG and JL analyzed the sequencing data. HG, ZG, and DX wrote an initial version of the manuscript. All authors read and approved the final manuscript.

Funding

This study was supported by the National Natural Science Foundation of China (grant no. 81371847).

Availability of data and materials

The datasets of this article are included within the manuscript and its supplementary material. All the RNA-seq raw data were submitted to the National Centre for Biotechnology Information (NCBI). Sequence Read Archive with a BioProject ID: PRJNA843865.

Declarations

Ethics approval and consent to participate

Not applicable.

Consent for publication

Not applicable.

Competing interests

The authors declare that there are no competing interests.

Received: 22 June 2022 Accepted: 13 September 2022
Published online: 01 October 2022

References

1. Singh M, Suryanshu Kanika, Singh G, Dubey A, Chaitanya RK. *Plasmodium's* journey through the *Anopheles* mosquito: a comprehensive review. Biochimie. 2021;181:176–90.
2. Weaver SC, Charlier C, Vasilakis N, Lecuit M. Zika, Chikungunya, and other emerging vector-borne viral diseases. Annu Rev Med. 2018;69:395–408.
3. Lobl M, Thieman TK, Clarey D, Higgins S, Trowbridge RM, Hewlett A, et al. What's eating you? *Culex* mosquitoes and West Nile virus. Cutis. 2021;107:244–7.
4. Aardema ML, vonHoldt BM, Fritz ML, Davis SR. Global evaluation of taxonomic relationships and admixture within the *Culex pipiens* complex of mosquitoes. Parasite Vectors. 2020;13:8.
5. Gomes B, Sousa CA, Vicente JL, Pinho L, Calderón I, Arez E, et al. Feeding patterns of molestus and pipiens forms of *Culex pipiens* (Diptera: Culicidae) in a region of high hybridization. Parasite Vectors. 2013;6:93.
6. Jaffar-Bandjee M, Steinmann T, Krijnen G, Casas J. Insect pectinate antennae maximize odor capture efficiency at intermediate flight speeds. P Natl Acad Sci USA. 2020;117:28126–33.
7. Eberl DF. Feeling the vibes: chordotonal mechanisms in insect hearing. Curr Opin Neurobiol. 1999;9:389–93.
8. McMeniman CJ, Corfas RA, Matthews BJ, Ritchie SA, Vosshall LB. Multimodal integration of carbon dioxide and other sensory cues drives mosquito attraction to humans. Cell. 2014;156:1060–71.
9. Wada-Katsumata A, Schal C. Antennal grooming facilitates courtship performance in a group-living insect, the German cockroach *Blattella germanica*. Sci Rep-UK. 2019;9:2942.
10. Raji JI, DeGennaro M. Genetic analysis of mosquito detection of humans. Curr Opin Insect Sci. 2017;20:34–8.
11. Chen Q, Pei D, Li J, Jing C, Wu W, Man Y. The antenna transcriptome changes in mosquito *Anopheles sinensis*, pre- and post- blood meal. PLoS ONE. 2017;12:e0181399.
12. Gu ZY, Gao HT, Yang QJ, Ni M, Li MJ, Xing D, et al. Screening of olfactory genes related to blood-feeding behaviors in *Culex quinquefasciatus* and *Culex pipiens molestus* by transcriptome analysis. PLoS Neglect Trop D. 2022;16:e0010204.
13. Sanford JL, Shields VD, Dickens JC. Gustatory receptor neuron responds to DEET and other insect repellents in the yellow-fever mosquito *Aedes aegypti*. Die Naturwissenschaften. 2013;100:269–73.
14. Carvalho DO, Chuffi S, Ioshino RS, Marques ICS, Fini R, Costa MK, et al. Mosquito pornoscopy: observation and interruption of *Aedes aegypti* copulation to determine female polyandric event and mixed progeny. PLoS ONE. 2018;13:e0193164.
15. Lombardo F, Salvemini M, Fiorillo C, Nolan T, Zwiebel LJ, Ribeiro JM, et al. Deciphering the olfactory repertoire of the tiger mosquito *Aedes albopictus*. BMC Genomics. 2017;18:770.
16. Saltin BD, Matsumura Y, Reid A, Windmill JF, Gorb SN, Jackson JC. Material stiffness variation in mosquito antennae. J R Soc Interface. 2019;16:20190049.
17. Dehghan H, Sadraei J, Moosa-Kazemi SH, Baniani NA, Nowruzi F. The molecular and morphological variations of *Culex pipiens complex* (Diptera: Culicidae) in Iran. J Vector Dis. 2013;50:111–20.
18. Tahir HM, Kanwal N, Mehwish. The sequence divergence in cytochrome C oxidase I gene of *Culex quinquefasciatus* mosquito and its comparison with four other *Culex* species. Mitochondrial DNA A DNA Mapp Seq Anal. 2016;27:3054–7.
19. Kim D, Paggi JM, Park C, Bennett C, Salzberg SL. Graph-based genome alignment and genotyping with HISAT2 and HISAT-genotype. Nat Biotechnol. 2019;37:907–15.

20. Behura SK, Lobo NF, Haas B, deBruyn B, Lovin DD, Shumway MF, et al. Complete sequences of mitochondria genomes of *Aedes aegypti* and *Culex quinquefasciatus* and comparative analysis of mitochondrial DNA fragments inserted in the nuclear genomes. Insect Biochem Molec. 2011;41:770–7.
21. O'Leary NA, Wright MW, Brister JR, Ciufo S, Haddad D, McVeigh R, et al. Reference sequence (RefSeq) database at NCBI: current status, taxonomic expansion, and functional annotation. Nucleic Acids Res. 2016;44:D733-745.
22. Kovaka S, Zimin AV, Pertea GM, Razaghi R, Salzberg SL, Pertea M. Transcriptome assembly from long-read RNA-seq alignments with stringTie2. Genome Biol. 2019;20:278.
23. Mistry J, Chuguransky S, Williams L, Qureshi M, Salazar GA, Sonnhammer ELL, et al. Pfam: the protein families database in 2021. Nucleic Acids Res. 2021;49:D412-d419.
24. The Gene Ontology resource. enriching a Gold mine. Nucleic Acids Res. 2021;49:D325-d334.
25. Mi H, Muruganujan A, Ebert D, Huang X, Thomas PD. PANTHER version 14: more genomes, a new PANTHER GO-slim and improvements in enrichment analysis tools. Nucleic Acids Res. 2019;47:D419-d426.
26. Kanehisa M, Sato Y, Kawashima M. KEGG mapping tools for uncovering hidden features in biological data. Protein Sci. 2022;31:47–53.
27. Love MI, Huber W, Anders S. Moderated estimation of fold change and dispersion for RNA-seq data with DESeq2. Genome Biol. 2014;15:550.
28. Wu T, Hu E, Xu S, Chen M, Guo P, Dai Z, et al. clusterProfiler 4.0: a universal enrichment tool for interpreting omics data. Innovation. 2021;2:100141.
29. Yu G, Wang LG, Han Y, He QY. clusterProfiler: an R package for comparing biological themes among gene clusters. OMICS. 2012;16:284–7.
30. Szklarczyk D, Gable AL, Nastou KC, Lyon D, Kirsch R, Pyysalo S, et al. The STRING database in 2021: customizable protein-protein networks, and functional characterization of user-uploaded gene/measurement sets. Nucleic Acids Res. 2021;49:D605-d612.
31. Shannon P, Markiel A, Ozier O, Baliga NS, Wang JT, Ramage D, et al. Cytoscape: a software environment for integrated models of biomolecular interaction networks. Genome Res. 2003;13:2498–504.
32. Chin CH, Chen SH, Wu HH, Ho CW, Ko MT, Lin CY. cytoHubba: identifying hub objects and sub-networks from complex interactome. BMC Syst Biol. 2014;8:S11.
33. Schmittgen TD, Livak KJ. Analyzing real-time PCR data by the comparative C(T) method. Nat Protoc. 2008;3:1101–8.
34. Bubner B, Gase K, Baldwin IT. Two-fold differences are the detection limit for determining transgene copy numbers in plants by real-time PCR. BMC Biotechnol. 2004;4:14.
35. Athrey G, Popkin-Hall Z, Cosme LV, Takken W, Slotman MA. Species and sex-specific chemosensory gene expression in *Anopheles coluzzii* and *An. quadriannulatus* antennae. Parasite Vectors. 2020;13:212.
36. Xu P, Wen X, Leal WS. CO (2) per se activates carbon dioxide receptors. Insect Biochem Molec. 2020;117:103284.
37. Pelletier J, Leal WS. Characterization of olfactory genes in the antennae of the Southern house mosquito *Culex quinquefasciatus*. J Insect Physiol. 2011;57:915–29.
38. Pelletier J, Leal WS. Genome analysis and expression patterns of odorant-binding proteins from the Southern House mosquito *Culex pipiens quinquefasciatus*. PLoS ONE. 2009;4:e6237.
39. Becker N, Jöst A, Weitzel T. The *Culex pipiens* complex in Europe. J Am Mosquito Contr. 2012;28:53–67.
40. Luande VN, Eklöf D, Lindström A, Nyanjom SG, Evander M, Lilja T. The Human Biting *Culex pipiens* Bioform molestus detected in several areas in Southern Sweden. Vector-Borne Zoonot. 2020;20:936–8.
41. Asigau S, Salah S, Parker PG. Assessing the blood meal hosts of *Culex quinquefasciatus* and *Aedes taeniorhynchus* in Isla Santa Cruz. Galápagos Parasite Vectors. 2019;12:584.
42. David JP, Ismail HM, Chandor-Proust A, Paine MJ. Role of cytochrome P450s in insecticide resistance: impact on the control of mosquito-borne diseases and use of insecticides on Earth. Philos T R Soc B. 2013;368:20120429.
43. Pavek P, Dvorak Z. Xenobiotic-induced transcriptional regulation of xenobiotic metabolizing enzymes of the cytochrome P450 superfamily in human extrahepatic tissues. Curr Drug Metab. 2008;9:129–43.
44. Knutsson S, Engdahl C, Kumari R, Forsgren N, Lindgren C, Kindahl T, et al. Noncovalent inhibitors of mosquito Acetylcholinesterase 1 with resistance-breaking potency. J Med Chem. 2018;61:10545–57.
45. Komagata O, Kasai S, Tomita T. Overexpression of cytochrome P450 genes in pyrethroid-resistant *Culex quinquefasciatus*. Insect Biochem Molec. 2010;40:146–52.
46. Zhao M, Dong Y, Ran X, Wu Z, Guo X, Zhang Y, et al. Point mutations associated with organophosphate and carbamate resistance in Chinese strains of *Culex pipiens quinquefasciatus* (Diptera: Culicidae). PLoS ONE. 2014;9:e95260.
47. Lv Y, Wang W, Hong S, Lei Z, Fang F, Guo Q, et al. Comparative transcriptome analyses of deltamethrin-susceptible and -resistant *Culex pipiens pallens* by RNA-seq. Mol Genet Genomics. 2016;291:309–21.
48. Li CX, Guo XX, Zhang YM, Dong YD, Xing D, Yan T, et al. Identification of genes involved in pyrethroid-, propoxur-, and dichlorvos- insecticides resistance in the mosquitoes, *Culex pipiens complex* (Diptera: Culicidae). Acta Trop. 2016;157:84–95.
49. Sawabe K, Moribayashi A. Lipid utilization for ovarian development in an autogenous mosquito, *Culex pipiens molestus* (Diptera: Culicidae). J Med Entomol. 2000;37:726–31.
50. Ma Z, Liu J, Guo X. A retinal-binding protein mediates olfactory attraction in the migratory locusts. Insect Biochem Molec. 2019;114:103214.
51. Masai I, Okazaki A, Hosoya T, Hotta Y. *Drosophila* retinal degeneration A gene encodes an eye-specific diacylglycerol kinase with cysteine-rich zinc-finger motifs and ankyrin repeats. P Natl Acad Sci USA. 1993;90:11157–61.
52. Masai I, Suzuki E, Yoon CS, Kohyama A, Hotta Y. Immunolocalization of Drosophila eye-specific diacylgylcerol kinase, rdgA, which is essential for the maintenance of the photoreceptor. J Neurobiol. 1997;32:695–706.
53. Choi JY, Choi CY. Gonadotropin-releasing hormone-independent effects of recombinant vertebrate ancient long opsin in the goldfish *Carassius auratus* reveal alternative reproduction pathways. Fish Physiol Biochem. 2020;46:1219–27.
54. Sarkar H, Moosajee M. Retinol dehydrogenase 12 (RDH12): Role in vision, retinal disease and future perspectives. Exp Eye Res. 2019;188:107793.
55. Hofmann L, Tsybovsky Y, Alexander NS, Babino D, Leung NY, Montell C, et al. Structural insights into the drosophila melanogaster retinol dehydrogenase, a member of the short-chain dehydrogenase/reductase family. Biochemistry-US. 2016;55:6545–57.
56. Wakakuwa M, Arikawa K, Ozaki K. A novel retinol-binding protein in the retina of the swallowtail butterfly. Papilio xuthus J Biochem. 2003;270:2436–45.
57. Noy N. Retinoid-binding proteins: mediators of retinoid action. J Biochem. 2000;3:481–95.
58. Kouchmeshky A, Goodman T, Whiting A, McCaffery P. Tissue localization of retinoic acid receptor (*RAR*) active drugs. Method Enzymol. 2020;637:513–38.
59. Liu N, Wang Y, Li T, Feng X. G-Protein Coupled Receptors (GPCRs): signaling pathways, characterization, and functions in insect physiology and toxicology. Int J Mol Sci. 2021;22:5260.
60. Li T, Liu N. The function of G-protein-coupled receptor-regulatory cascade in Southern house mosquitoes (Diptera: Culicidae). J Med Entomol. 2018;55:862–70.
61. Soliman MA, Seif AI, Hassan AN, Abdel-Hamid ME, Mansour MA, Gad AM. Nutritional reserves in autogenous and anautogenous populations of *Culex pipiens* and *Aedes caspius* (Diptera: Culicidae). J Egypt Soc Parasitol. 1995;25:499–507.
62. Su T, Mulla MS. Nutritional reserves, body weight, and starvation tolerance of autogenous and anautogenous strains of *Culex tarsalis* (Diptera:Culicidae). J Med Entomol. 1997;34:68–73.
63. Kim MS, Smith DP. The invertebrate odorant-binding protein LUSH is required for normal olfactory behavior in *Drosophila*. Chem Senses. 2001;26:195–9.
64. Kim MS, Repp A, Smith DP. LUSH odorant-binding protein mediates chemosensory responses to alcohols in *Drosophila melanogaster*. Genetics. 1998;150:711–21.
65. Lien NTK, Ngoc NTH, Lan NN, Hien NT, Tung NV, Ngan NTT, et al. Transcriptome sequencing and analysis of changes associated with insecticide resistance in the dengue mosquito (*Aedes aegypti*) in Vietnam. Am J Trop Med Hyg. 2019;100:1240–8.

66. Belyaeva OV, Korkina OV, Stetsenko AV, Kim T, Nelson PS, Kedishvili NY. Biochemical properties of purified human retinol dehydrogenase 12 (RDH12): catalytic efficiency toward retinoids and C9 aldehydes and effects of cellular retinol-binding protein type I (CRBPI) and cellular retinaldehyde-binding protein (CRALBP) on the oxidation and reduction of retinoids. Biochemistry-US. 2005;44:7035–47.
67. Marchette LD, Thompson DA, Kravtsova M, Ngansop TN, Mandal MN, Kasus-Jacobi A. Retinol dehydrogenase 12 detoxifies 4-hydroxynonenal in photoreceptor cells. Free Radical Bio Med. 2010;48:16–25.

Publisher's Note